Journal of Ceramic Processing Research. Vol. 16, No. 2, pp. 188~192 (2015)

J O U R N A L O F
Ceramic Processing Research

Structural and electrical properties of semiconducting $YBa_2Cu_3O_{6+x}$ thin film by sol-gel for uncooled infrared detectors

Tae-Ho Lee, Sung-Gap Lee* and Jae-Woon Jeong

Dept. of Ceramic Engineering, Eng. Res. Insti., Gyeongsang National University, Jinju-Si, Korea

Uncooled pyroelectric infrared detectors based on semiconducting $YBa_2Cu_3O_{6+x}$ (YBCO) thin films were investigated. YBCO precursor solutions were prepared using the sol-gel method and YBCO films were fabricated by spin coating. The structural and electrical properties at varying annealing temperatures were studied. From differential thermal analysis and thermogravimetry (DTA-TG) results, an endothermic peak was observed at around 700 °C, due to the formation of a tetragonal phase. The crystal structure of the YBCO film annealed at 600 °C~800 °C was a polycrystalline tetragonal phase. All specimens displayed a second phase ($BaCO_3$). The YBCO film sintered at 700 °C showed a small grain size and smooth surface. The temperature resistance coefficient (TCR), responsivity and detectivity of the YBCO film sintered at 700 °C were −2.76%/°C at room temperature, 36.17V/W and 4.77×10^6 cmHz1/2W^{-1}, respectively.

Key words: Thin films, Sol-gel growth, Electrical properties, Electron microscopy(SEM).

Introduction

Infrared (IR) imaging has the potential to play an equally important role in commercial applications in medical, military and transportation systems. In particular, automobiles equipped with IR imaging capabilities have been envisioned for the near future. This technology has the potential to tremendously improve personal safety by allowing better vision at night and under adverse weather conditions. Infrared images in automobiles may also be an enabling technology for "intelligent superhighways". However, IR imaging systems currently used by the military or medical industry are too expensive and require a cooling system for consumer applications [1-2]. Recently, uncooled and inexpensive IR imaging detectors have been studied for application in various sensor devices [3].

Bolometer IR detectors detect changes in the electrical resistance of a thermally isolated material due to temperature change using the incident IR signal. The bolometer IR detectors studied have been mainly the resistive type, which detect changes in the resistance of metal, semiconductor and superconductor materials. Bolometer IR detectors are characterized by their simple manufacturing processes and are capable of operating at room temperature [4-6].

Recently, bolometer IR detectors using titanium, vanadium oxide and $YBa_2Cu_3O_{6+x}$ (YBCO) thin films have been studied for their potential applications. However, titanium thin films, which have a temperature coefficient of resistance of 0.28%/°C, display a low sensitivity performance for the incident IR. Single-composition vanadium oxide thin films are difficult to produce by the sputtering or implantation method due to compositional instability [7]. YBCO is known as a high-temperature superconductor. The optical and electronic properties of $YBa_2Cu_3O_{6+x}$ are determined by its oxygen stoichiometry. For $x \approx 1$, YBaCuO possesses an orthorhombic crystal structure, exhibits metallic conductivity, and becomes superconductive upon cooling below its critical temperature. As x decreases to 0.5, the crystal undergoes a phase transition to a tetragonal structure and exhibits semiconducting conductivity characteristics as it exists in a Fermi glass state. As x decreases further below 0.3 YBaCuO becomes a Hubbard insulator with a well defined energy gap on the order of 1.5 eV. This work utilizes the semiconducting phase of the material [8]. Semiconducting YBCO thin films possess a high pyroelectric coefficient at room temperature, two hundred times greater than other thin film materials. Different materials used as bolometers, including vanadium oxide VO_x [9-10], amorphous Si [11-12], doped poly Si [13-14], and poly Si-Ge alloys [15-16], have been reported. YBCO films have a temperature coefficient of resistance of 3.5 ~ 4%/°C and low leakage current densities. Therefore, YBCO films are suitable for application in bolometer IR detectors [17-18].

In this study, semiconducting YBCO thin films were prepared using the sol-gel method, which involved spin-coating in a $Pt/Ti/SiO_2/Si$ substrate using YBCO alkoxide solutions. We also investigated the structural and electrical properties of YBCO thin films at varying annealing temperatures for application in IR detectors.

*Corresponding author:
Tel : +82-10-2686-4427
Fax: +82-55-772-1689
E-mail: lsgap@gnu.ac.kr

Experimental Procedure

Using the sol-gel method, YBCO precursor solutions were prepared from the starting materials yttrium acetate tetrahydrate [$Y(CH_3COO)_3 \cdot 4H_2O$], copper acetate monohydrate [$Cu(CH_3COO)_2 \cdot H_2O$], and barium hydroxide [$Ba(OH)_2 8H_2O$], in addition to the solvent propionic acid and propylamine. The stoichiometric molar ratio of yttrium acetate, barium hydroxide and copper acetate is 1 : 2 : 3. The oxide concentration of the solution is 0.3 mol/L, with a 6 : 1 ratio of propionic acid to propylamine. Diethanolamine is also used to increase the wetting and reduce the surface tension of the solution above the polished substrate. The YBCO precursor solution was passed through a syringe filter and spin-coated on the Pt(200 nm)/Ti(10 nm)/SiO_2(300 nm)/p-Si<100> substrates using a spinner operator at 3,000rpm for 20 sec to form the first layer. These YBCO films were dried at 200 ~ 250 °C for several minutes in air. Generally, one coating gives a thickness of 0.06 ~ 0.08 μm. This coating/drying procedure was repeated several times to obtain the desired thickness (approximately 0.269 ~ 0.401 μm). The multicoated thin films were dried at 500 °C for 1 ~ 3 h to remove the organic materials, and annealed at 600 ~ 800 °C for 1 h in an Ar/O_2 (50 : 50) atmosphere to crystallize them into a tetragonal structure. The crystalline structures of the YBCO thin films were analyzed using a D8 Discover & General Area Detector X-ray Diffraction System (GADDS-SN002623, XRD) with CuKa emission. The surface and cross-sectional microstructures of the films were examined using field-emission scanning electron microscopy (FE-SEM). The electrodes were fabricated by screen-printing the Ag paste. The electrical properties of the specimens were measured using an LCR meter (Fluke 6306, USA) and an electrometer (Keithley 6517A, USA) for IR detector applications.

Results and Discussion

Measurements from the differential thermal analysis (DTA) and thermogravimetry analysis (TGA) curves of the YBCO solution were collected, and the results are shown in Fig. 1. An endothermic peak due to the evaporation of adsorbed water and solvent was observed at around 150 °C. Due to the decomposition of organic residues, exothermic peaks were observed in the temperature range of 400 °C. The weight loss at around 720 °C was attributed to the decomposition of barium carbonate, which formed during heating [19]. In addition, the small exothermic peak at around 800 °C can be attributed to the formation of a single Y_2O_3 phase [20]. Due to the formation of the polycrystalline YBCO phase, exothermic peaks were observed at around 700 °C because not much weight loss could be observed in the TGA curve.

Fig. 2 shows the X-ray diffraction patterns of YBCO thin films printed on a Pt/Ti/SiO_2/Si substrate at varying annealing temperatures. YBCO films annealed at 600 °C and 650 °C displayed a second and unreacted phase such as $BaCuO_2$ or $BaCO_3$ because of the low annealing temperature. The films sintered at 700 °C showed the typical XRD pattern of the tetragonal polycrystalline structure $YBa_2Cu_3O_{6.5}$ and a second phase was also observed. However, the film sintered at 800 °C showed a second phase such as $BaCO_3$ or CuO due to the excess annealing temperature.

Fig. 3 shows surface SEM micrographs of YBCO films at varying annealing temperatures. The grain size decreased with an increase in annealing temperature, and the YBCO film sintered at 700 °C showed a small grain size and smooth surface. The YBCO films annealed at 600 °C and 650 °C showed the small grain with large grain due to the low annealing temperature. The film annealed at 800°C displayed pores and cracks due to the high annealing temperature. The big grain size was due to the formation of a second phase such as $BaCO_3$, CuO or $BaCuO_2$. The second phase decreased with an increase in annealing temperature. Crystallization of YBCO thin films was severely affected by the annealing temperature, as shown in Fig. 2.

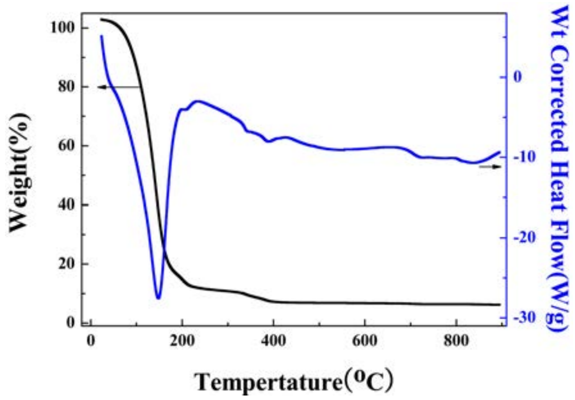

Fig. 1. DTA/TG curves of sol-gel derived $YBa_2Cu_3O_{6+x}$ solution.

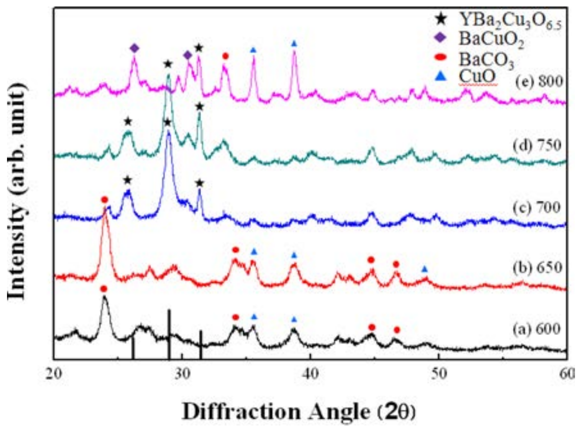

Fig. 2. XRD patterns of $YBa_2Cu_3O_{6+x}$ thin film as a function of annealing temperature; (a)600 °C, (b)650 °C, (c)700 °C, (d)750 °C and (e)800 °C.

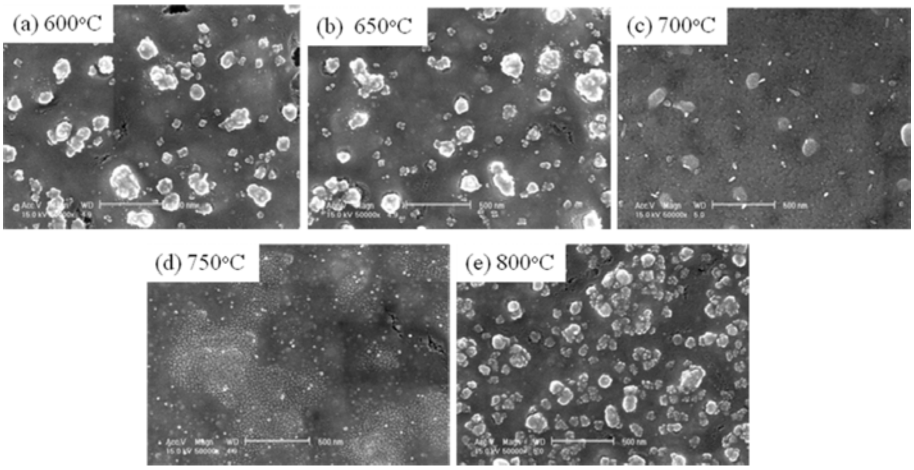

Fig. 3. Surface SEM micrographs of $YBa_2Cu_3O_{6+x}$ thin film as a function of annealing temperature; (a)600 °C, (b)650 °C, (c)700 °C, (d)750 °C and (e)800 °C.

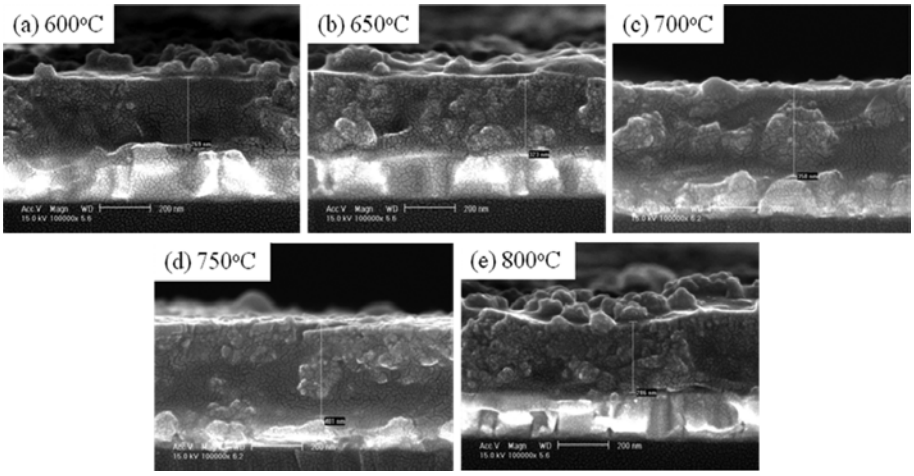

Fig. 4. Cross-sectional SEM micrographs of $YBa_2Cu_3O_{6+x}$ thin film as a function of annealing temperature; (a)600 °C, (b)650 °C, (c)700 °C, (d)750 °C and (e)800 °C.

Fig. 4 shows cross-sectional SEM micrographs of YBCO thin films at varying annealing temperatures. The thickness of all films was approximately 0.269 ~ 0.401 μm, and film thickness was not dependent on the annealing temperature. All films displayed a relatively flat surface morphology with the pores distributed inside the films. Typically, the pores in IR detector materials prevent dispersion of the incident IR, decreasing the sensitivity of IR detectors. Thus, in order to obtain good sensitivity properties, the films should have a dense and void-free grain structure.

Fig. 5 shows the temperature coefficient of resistance (TCR) of YBCO thin films at varying annealing temperatures. All YBCO films displayed NTCR (negative temperature coefficient of resistance) properties, which means that electrical resistance decreased with an increase in temperature, typical of semiconductor materials. Electrical resistance and TCR increased with an increase in annealing temperature, and the YBCO films annealed at 700 °C showed the highest values of 15.96MΩ and −2.76%/°C at room temperature, respectively. This is due to the small grain size and smooth surface with an increase in annealing temperature, as shown in Fig. 3. However, in the films annealed at 800 °C, electrical resistance and TCR decreased with an increase in the second phase, pores and cracks.

A sensing element performance evaluation system, as shown in Fig. 6, was used to evaluate the responsivity and detectivity performance of the YBCO thin film IR devices, and a blackbody source furnace at a temperature of 500 °C was used to measure the pyroelectric characteristics of YBCO thin films in the system. The measurement set-up is shown in Fig. 6. Fig. 7 and Fig. 8 show the voltage responsivity and detectivity of YBCO thin films at varying annealing temperatures. Voltage responsivity, Rv, which is the ratio of the output voltage by the pyroelectric effect to the incident radiant power, was calculated using Eq. (1).

$$R = \frac{V_s}{EA_D}[V/W] \quad (1)$$

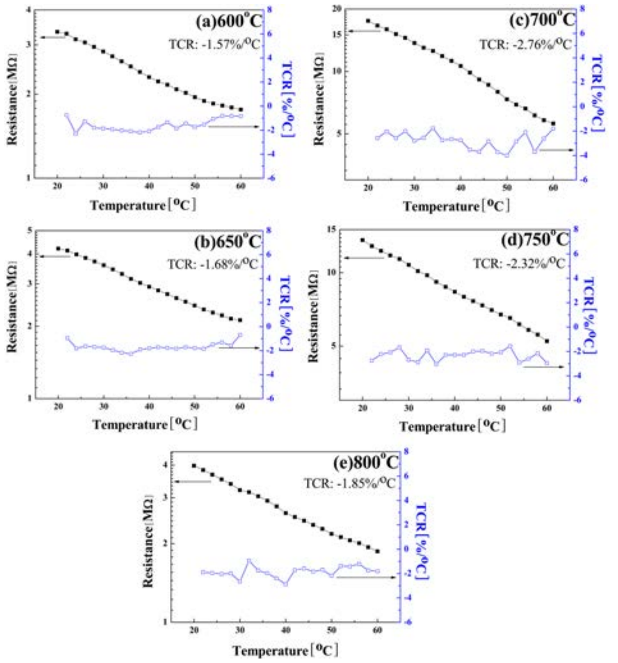

Fig. 5. Resistance and TCR of $YBa_2Cu_3O_{6+x}$ thin film as a function of annealing temperature; (a)600 °C, (b)650 °C, (c)700 °C, (d)750 °C and (e)800 °C.

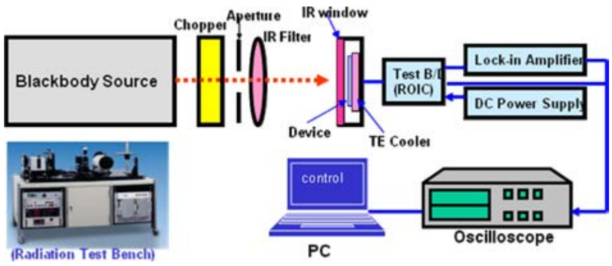

Fig. 6. Measurement set-up for IR device characterization.

Table. 1. Measuring parameters.

BBS Temperature	500 °C
Chopper Frequency	15 Hz
BBS Aperture	0.6"
Bias Voltage	1V
Gain	25
Filter	9.46 µm/9.00 ~ 10.0 µm
Distance	3 cm

where VS is the signal output, VN is the noise output, AD is the detector area, E is the irradiance, and Δ f is the effective radiation bandwidth. Detectivity, D*, which is the signal-to-noise ratio of the detector when an incident infrared beam is radiated per unit area, was calculated using Eq. (2).

$$D^* = \frac{\sqrt{\Delta f A_D}}{NEP}[cmHz1/2W^{-1}]$$

$$NEP = EA_D\left(\frac{V_N}{V_S}\right) \qquad (2)$$

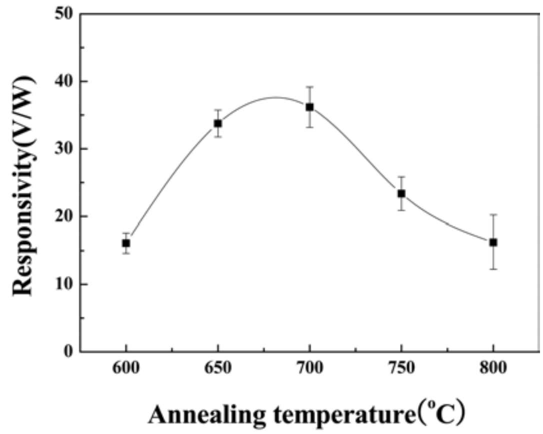

Fig. 7. Responsivity of $YBa_2Cu_3O_{6+x}$ thin films with variation of annealing temperature.

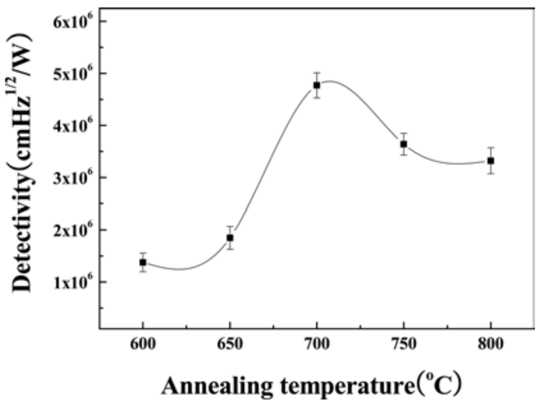

Fig. 8. Detectivity of $YBa_2Cu_3O_{6+x}$ thin films with variation of annealing temperature.

Table 1 shows the measuring parameters for responsivity and detectivity.

The YBCO films annealed at 700 °C displayed maximum values of 36.17[V/W] and 4.77 × 106[cmHz1/2W^{-1}], respectively. The maximum voltage responsivity and detectivity were due to the high TCR and electrical resistance, as shown in Eq. (1). Furthermore, the semiconducting YBCO single phase displayed excellent electrical properties, as shown in Fig. 5.

Conclusions

In this study, we fabricated semiconducting YBCO thin films using the spin-coating method. The YBCO thin films were annealed at 600 ~ 800 °C. Crystallization of the YBCO thin films was severely affected by the annealing temperature and the films annealed at 700 °C displayed a tetragonal polycrystalline structure. Decomposition of barium carbonate occurred at 720 °C and the formation of a polycrystalline YBCO phase occurred at around 700 °C. Pores in the IR detector materials prevent the dispersion of the incident IR, decreasing the sensitivity of the IR detectors. The temperature resistance coefficient, responsivity and detectivity of the YBCO film sintered at 700 ^{o}C were $-2.76\%/^{o}C$ at room temperature, 36.17V/W and 4.77×10^6 cmHz1/2W^{-1}, respectively.

Acknowledgments

This work was supported by the Korea Research Foundation (KRF) grant funded by the Korea government (MEST) (No. 03-2011-0223).

References

1. F. Niklaus, C. Vieider and H. Jacobsen, Proc. SPIE 6836 (2007) 0D1.
2. L. Luo, M. E. Hawley, C. J. Maggiore, R. C. Dye and R. E. Muenchausen, Appl. Phys. Lett. 62 (1993) 485.
3. P.-Y. Chu and R. C. Buchaman, J. Mater. Res. 8 (1993) 2134.
4. P. C. Mcintyre, M. J. Cima, J. A. Smith, R. B. Hallock, M. P. Siegal and J. M. Phillips, J. appl. Phys. 71 (1992) 1868.
5. A. Jahanzeb, C. M. Travers, D. P. Butler, Z. Celik-Butler and J. E. Gray, Appl. Phys. Lett. 70 (1997) 3495.
6. A. Aligia and J. Garces, Phys. Rev. B 49 (1994) 524.
7. N. A. Khan, M. Z. Iqbal and N. Baber, Solid State Commun. 92 (1994) 607.
8. A. Dasgupta, S. Ghosh, and S, Ray, J. Mater. Sci. Lett. 14 (1995) 1037.
9. S. Mathews, Thermal imaging on the rise, Laser Focus World 40 (2004)105-107.
10. W. Radford, D. Murphy, M. Ray, S. Propst, A. Kennedy, J. Kojiro, J. Woolayaw, K. Soch, R. Coda, G. Lung, E. Moody, D. Gleichman, S. Baur, SPIE Proc. 2746 (1996) 82-92.
11. J. Brady, T. Schimert, D. Ratcliff, R. Gooch, B. Ritchey, P. McCardel, K. Rachels, S. Ropson, M. Wand, M. Weinstein, J. Wynn, SPIE Proc. 3689 (1999) 161-167.
12. T. Schimert, D. Ratcliff, J. Brady, S. Ropson, R. Gooch, B. Ritchey, P. McCardel, K. Rachels, M. Wand, M. Weinstein, J. Wynn, SPIE Proc. 3713 (1999) 101-111.
13. M.S. Liu, J.S. Haviland, C.J. Yue, Intergrated Infrared Sensitive Bolometers, Patent No. US005260225A (1992).
14. P. Fiorini, S. Sedky, M. Caymax, C. Baert, Patent No. US009194722B1 (2001).
15. J. Wauters, Laser Focus World 33 (1997) 145-148.
16. A. Tanaka, S. Matsumoto, N. Tsukamoto, S. Itoh, T. Endoh, A. Nakazato, Y. Kumazawa, M. Hijikawa, H. Gotoh, T. Tanaka, N. teranishi, Tech. Digest, in: International Conference on Solid-State Sensors and Actuators and Eurosensors IX, vol.2, Stockholm, Sweden, June 25-29 (1995) 632-635.
17. M. Longhin, A. J. Kreisler, and A. F. Degardin, Materials Science Forum 587 (2008) 273.
18. A. Mahmood, D. P. Butler, and Z. Celik-Butler, Sens. Actuators A, 132 (2006) 452.
19. T. Hayashi, H. Shinozaki, K. Sasaki, Jap. J. Appl. Phys. 37 5232 (1998).
20. T. T. Thuy, S. Hoste, G. G. Herman, K. De Buysser, P. Lommens, J. Feys, D. Vandeput, I. Van Driessche, J Sol-Gel Sci Technol, 52 (2009) 124.